RAPID COMMUNICATIONS IN MASS SPECTROMETRY
Rapid Commun. Mass Spectrom. 2009; **23**: 3183–3193
Published online in Wiley InterScience (www.interscience.wiley.com) DOI: 10.1002/rcm.4222

RCM

Development of an advanced on-line position-specific stable carbon isotope system and application to methyl *tert*-butyl ether

Caroline Gauchotte[1,4]*, Gwen O'Sullivan[2], Simon Davis[3] and Robert M. Kalin[1]

[1]Department of Civil Engineering, University of Strathclyde, John Anderson Building, Glasgow G4 0NG, UK
[2]Trium Environmental Solutions Inc., Cochrane, Alberta, T4C 0A4, Canada
[3]Compact Science Systems, Lymedale Business Centre, Newcastle-under-Lyme ST5 9FQ, UK
[4]School of Planning, Architecture and Civil Engineering, Queen's University Belfast, David Keir Building, Belfast BT9 5AG, UK

Received 14 May 2009; Revised 21 July 2009; Accepted 22 July 2009

We present an advanced system for on-line position-specific carbon isotope analysis. The main limitation of on-line intramolecular isotope ratio measurements has been that optimal pyrolytic fragments are obtained mostly at temperatures where the analyte has not completely reacted. As a result of undetermined isotopic fractionation, the isotopic signatures of the pyrolysis products are not strictly equal to these of the equivalent moieties in the parent molecule. We designed a pyrolytic unit in which both temperature and reaction time are variable parameters, enabling determination of the enrichment factor of the pyrolysis at optimal temperature by construction of a Rayleigh plot. In the case of methyl *tert*-butyl ether (MTBE) presented here, a 'pre-pyrolysis' fractionation of MTBE leading to a depletion of 0.9‰ was discovered and the enrichment factor of the optimal pyrolysis reaction was determined at −1.7‰. Absolute $\delta^{13}C$ values of two functional groups of MTBE – the methoxy group and the 2-methylpropane group – could be determined with 95% confidence intervals of 0.4‰ and 0.5‰, respectively. Copyright © 2009 John Wiley & Sons, Ltd.

The introduction of continuous flow isotope ratio mass spectrometry (CF-IRMS) during the last decade has enabled the development of a new technique, which couples gas chromatography and isotope ratio mass spectrometry (GC-c-IRMS)[1–5] for on-line measurements of intermolecular isotopic variations at very low levels (nanomolar quantities). Compound-specific stable isotope analysis (CSIA) has become a routine technique in many areas including geochemistry,[6] pharmacology,[7] medicine[8] and forensic science.[9]

In Environmental Forensics, CSIA is fast becoming a major tool for the investigation of the origin and fate of environmental pollutants.[10,11] Because isotopic fractionation occurs during most (bio)chemical and physical processes, the stable isotopic signatures of an organic contaminant contain information about its history from synthesis to degradation. Synthesis pathway (natural and anthropogenic) conditions have been found to have a significant influence on the isotopic composition.[12–14] Studies of the environmental fate of contaminants have demonstrated that while non-degradative processes, such as volatilisation[14–19] and sorption,[20,21] have no significant effect on stable isotopic signatures, some microbial degradations may generate substantial isotopic fractionation. CSIA has, therefore, successfully been used for source allocation but it has also emerged as a method of choice for the detection, monitoring and quantification of environmental biodegradation[22–36] independently of mass losses due to weathering processes. Methods using the carbon and hydrogen CSIA data of contaminants have also been developed for the investigation of biodegradation pathways.[37–42] The combination of the carbon and hydrogen Rayleigh enrichment factors of biodegradations enables distinction between degradation mechanisms.[38–40] An alternative and potentially more powerful approach to the elucidation or the differentiation of degradation pathways is via the measurements of *intra*molecular isotopic variations.

Position-Specific Isotope Analysis (PSIA) determines the isotope ratios of different moieties in a molecule. PSIA can be carried out using either nuclear magnetic resonance (NMR) or IRMS techniques. NMR has been used for PSIA to estimate both deuterium and carbon 13 isotope shifts. Accurate measurements require very large sample sizes, which are often incompatible with environmental samples, particularly for carbon stable isotopes. Carbon PSIA using CF-IRMS works by breaking down a molecule into relevant fragments, giving access to the isotope signatures of various moieties in the molecule. Historically, PSIA was carried out by chemolysis, using carefully selected chemical reactions.[43–45] Off-line chemolysis presents disadvantages for field samples, such as possible uncontrolled isotopic fractionations due to the multiplication of sample preparation stages. Moreover, as for NMR, it requires sample sizes larger than those routinely available.

*Correspondence to: C. Gauchotte, Department of Civil Engineering, University of Strathclyde, John Anderson Building, Glasgow G4 0NG, UK.
E-mail: caroline.gauchotte@strath.ac.uk

A system coupling on-line pyrolysis and classic GC-c-IRMS (py-GC-c-IRMS) for *intra*molecular isotope analysis was first designed in 1997 by Corso and Brenna for applications in biology and biomedicine.[46] With this initial design, molecular cracking occurs by non-catalysed pyrolysis and as such the system is flexible and readily adaptable for a wide variety of volatile and semi-volatile compounds compatible with gas chromatography. The range of its applications has so far included alkanes,[47] toluene,[47] fatty acid methyl esters,[48] lactic acid,[49] and four amino acids.[50,51] Low molecular weight organic acids have also been investigated through similar systems for applications in environmental[52] and geoscience.[53] In most cases, the pyrolysis reaction is not quantitative.

Because isotopic fractionation may occur during non-quantitative reactions, the isotopic signatures of the pyrolysis products may not be equal to the isotopic signatures of the equivalent moieties in the parent molecule. Previous PSIA studies did not determine absolute *intra*molecular isotope ratios and the values were reported only as relative isotope ratios by comparison with chemically identical standards.[49–51]

The lack of absolute *intra*molecular isotope ratios limits the application of PSIA for Environmental Forensics because there is no means for interlaboratory comparisons of results. Brenna and co-workers[49] proposed a theoretical method to calculate *intra*molecular fractionation to overcome this problem. We report here, for the first time, the development of an on-line PSIA system equipped with an improved pyrolysis furnace that allows for adjustable temperatures and residence times to facilitate experimental evaluation and calculation of the pyrolysis isotopic fractionation.

This new method has been applied to methyl *tert*-butyl ether (MTBE), a synthetic compound which is globally added to gasoline to improve fuel performance and combustion efficiency. The increased production and use of MTBE have led to its detection in the environment; it has become a contaminant of concern due to its highly soluble nature and poor adsorption to soil. Understanding the origin and fate of MTBE is a topical issue in Environmental Forensics. Stable isotope analysis of MTBE has been applied to establish the occurrence of different biodegradation pathways of MTBE in the environment and the calculation of kinetic isotope rates has led to hypotheses on their mechanisms.[25,26,32,33,35,36,39] Two sites of attack have been hypothesised for the first stage of MTBE biodegradation depending on the microbial conditions: the central carbon atom of the 2-methylpropane group and the carbon atom of the methoxy group. Using off-line quantitative nucleophilic substitution, the heterogeneous carbon isotopic distribution between the two groups was recently reported.[39,41] The methoxy group was found to be highly depleted (around −35‰) relative to the *tert*-butyl group (−25‰). MTBE samples originating from different manufacturers but with the same overall $\delta^{13}C$ showed distinguishable $\delta^{13}C$ values for these two functional groups.[41]

MTBE is mainly produced by the reaction of methanol with isobutylene over a catalyst bed. The carbon atoms of the 2-methylpropane side of MTBE originate from the isobutylene while methanol is the carbon source for the methoxy group. Methanol is a commercially available compound that is produced either from natural gas, coal, the distillation of wood or the degradation of biomass. Isobutylene can be sourced from the mixed C4 streams, known as raffinate-1, generated as by-products in either steam cracking or fluid catalytic cracking of petroleum but also from the dehydrogenation of isobutane (2-methylpropane) or from the dehydration of *tert*-butyl alcohol.[56] The various potential origins of the raw materials mean that their carbon isotopic values may vary greatly.

The stable isotopic values of the different carbon atoms are also determined by the isotopic fractionation occurring during the production process; this fractionation will affect most the site of reaction, i.e. the central carbon atom of isobutylene. Parameters of the production process such as the catalysts used, reaction phases, pressures and temperatures vary from one production plant to another and may also vary from one batch to the next, rendering unique the associated isotopic fractionation. Position-specific isotope analysis has therefore the potential to link MTBE samples to the raw materials used for their production and their synthesis, and also to identify the sites of microbial attack.

We report here a method for the on-line PSIA of MTBE with direct quantification of the isotope effect to test the applicability of our hybrid, GC-pyrolysis (Py)-GC-time-of-flight mass spectrometry (TOFMS)/c-IRMS system for routine PSIA in Environmental Forensics. Accurate quantification of the pyrolysis isotopic fractionation was achieved by (i) assessment of isotopic fractionation internal to the system and not related to the pyrolysis, (ii) investigation of the pyrolysis temperature for optimal fragmentation, and (iii) calculation of the fractionation factor of the pyrolysis using the Rayleigh equation.

EXPERIMENTAL

Chemicals

MTBE (99.8% HPLC grade; Sigma Aldrich, St. Louis, MO, USA) and benzene (99.7% analytical grade; BDH, Poole, UK) were used without further purification.

Preparation of the standard solutions

Because benzene does not readily pyrolyse below 800°C, it was chosen as an internal standard. We prepared a MTBE/benzene (3:1, v/v) solution for the experiments.

For the calibration curve of MTBE vs. benzene for the IRMS studies, six solutions with a range of volumetric ratios between 3:1 and 1:4 were prepared.

MTBE/benzene solutions were stored in 2 mL vials, without headspace, with polypropylene screw caps with PTFE/silicone septa and kept at 4°C when not in use. Individual vials were never used for longer than a working day and volumes drawn for analysis were insufficient to allow headspace to appear. These precautions were taken to avoid differential evaporation of MTBE and benzene that could have changed the volumetric ratios and led to analytical uncertainty.

DOI: 10.1002/rcm

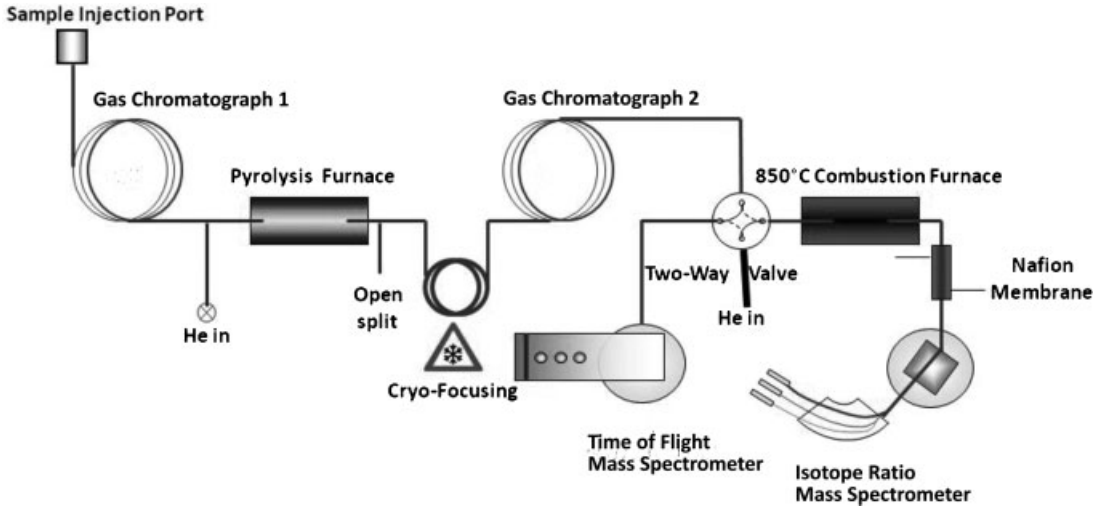

Figure 1. Schematic diagram of the GC-Py-GC-TOFMS/c-IRMS system. MTBE is pyrolysed at the outlet of the first gas chromatograph. It is cryo-focused with its pyrolysates before being injected into the second capillary column. A two-way valve directs the flow either to the time-of-flight mass spectrometer for structural analysis of the pyrolysates or to the isotope ratio mass spectrometer via the combustion furnace and a water trap (Nafion membrane) for carbon isotopic analysis.

Design of the GC-Py-GC-TOFMS/c-IRMS system

A schematic diagram of the GC-Py-GC-TOFMS/c-IRMS instrumentation is shown in Fig. 1. A description of the function and operation of the individual components of the system is given below.

Initial GC system

An initial gas chromatograph was used for the vaporisation and purification of MTBE. This unit was a CE 8000 Top equipped with a split/splitless injector (Thermoquest, Milan, Italy). For the analysis of MTBE, it was fitted with a 30 m *forte* BPX-vol capillary column (SGE, Ringwood, Victoria, Australia). The inlet pressure of the carrier gas helium was kept constant at 150 kPa while the temperature was maintained isothermal at 60°C. This ensured a constant flow rate. The injector was operated at 250°C in split mode with a 75:1 split ratio and a constant injection volume of 0.4 μL. The eluent of the initial gas chromatograph column passed to the pyrolysis unit.

Pyrolysis unit

In the pyrolysis unit described below the compound of interest was thermolysed without a catalyst in the gaseous phase.

The pyrolysis reactor was constructed of a quartz tube embedded in a temperature-controlled furnace. Five centimetres of the end of the capillary columns were threaded into the inlet of the quartz tube through a tee union. A secondary helium supply was connected to the third branch of the tee union (detailed in Fig. 2).

In previously reported on-line PSIA systems, the pyrolysis of the target compounds was optimised for pyrolysis temperature alone. We designed a pyrolysis unit that enabled us to also vary the pyrolysis reaction time by adding a controlled pressure of helium to the flow at the inlet of the furnace. To avoid the risk of backflushing, we placed an open-split at the outlet of the furnace. The residence time of the sample in the furnace depends on the dimension of the furnace and on the flow rate, which is controlled by the pressures and temperatures in the system. The head-pressure of the first gas chromatograph was kept constant while the open-split vented to atmospheric pressure. The pressures in both mass spectrometers were within the molecular flow range ($=<1\times10^{-3}$ mbar). All other

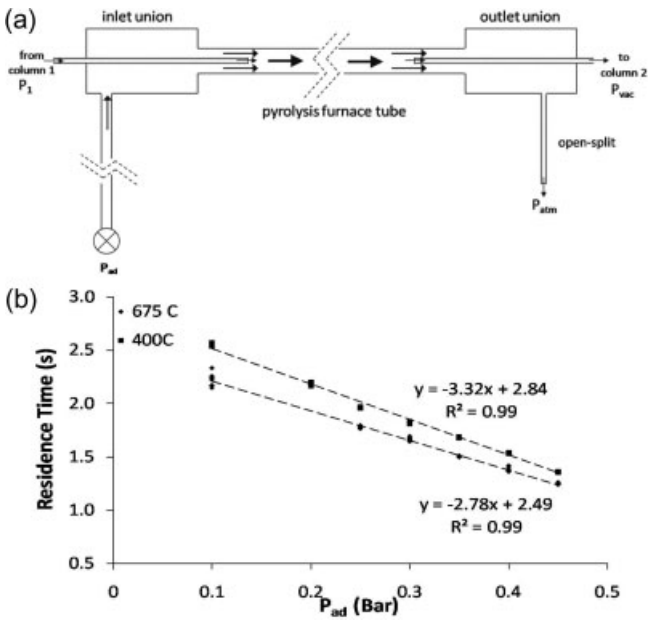

Figure 2. (a) Detail of the pyrolysis furnace. The inlet pressure in the first column is kept constant at P_1, the open-split opens to atmospheric pressure (P_{atm}), and the pressure in both mass spectrometers is within the molecular flow range ($=<1\times10^{-3}$ mbar) (P_{vac}). The pressure P_{ad} of the added helium controls the pressure differential and hence the flow rate in the furnace. (b) Plot of the residence time (calculated with the Hagen-Poiseuille equation) vs. the added helium pressure.

DOI: 10.1002/rcm

parameters (temperatures of the gas chromatograph ovens and dimensions of columns and capillaries) remained constant. The added helium pressure (P_{ad}) thus controlled the residence time.

To calculate the residence times, we measured the flow rate at the open-split for various values of P_{ad} (ranging from 0.1 to 0.4 bar). This was repeated with oven temperatures set at 400 and 675°C. Figure 2(b) is a plot of the residence times calculated from the measured flow rate using the Hagen-Poiseuille equation vs. the added helium pressure. The residence times were calculated using approximations for the dimensions of the fused-silica capillaries and capillary columns because the exact measurements were unknown. The residence time was found to be linearly related to the added helium pressure at both temperatures.

The flow rate at the open-split was not measured in further experiments. The linearity of the relationship of the added helium pressure against residence time was assumed, and the added helium pressure was utilised as a relative measurement of the residence time.

Cryo-focusing unit

The pyrolysis tube was connected to a custom-built cryo-focusing system which in turn was linked to the second gas chromatograph. The compound of interest and its pyrolysates were trapped and focused by the cryo-focusing system prior to injection into the second gas chromatograph.

The cyro-focusing unit was composed of a continuous piece of 250 μm i.d. capillary fed first through an 18 cm loop of nickel casing. This casing was layered with heating tape. Subsequently, the silica was passed through an 80 cm straight stainless steel tube sheathed in isolating tape. For the analysis of MTBE and its pyrolysates, the nickel loop was rapidly immersed into liquid nitrogen for a period of 11 min 30 s. This was carried out 6 min 30s before injection of the sample and for an additional 5 min after injection. Upon removal of the loop from the liquid nitrogen heat was applied via the heating tape to vaporise the trapped compounds.

Secondary GC system

In the second gas chromatograph, the products of the pyrolysis (pyrolysates) and the remaining reactant were separated.

The second chromatographic unit was a HP5890 (Hewlett Packard, Palo Alto, CA, USA). The injector was by-passed and the capillary from the pyrolysis unit was directly connected to the capillary column via a zero dead volume union. The inlet pressure was governed by the added helium pressure at the time of the vaporisation of the sample and its pyrolysates.

For the analysis of MTBE and its pyrolysates, the gas chromatograph was fitted with a 30 m Solgel-wax capillary column (SGE). The temperature was held at 55°C until the sample had been vaporised and then it was ramped to 185°C at a rate of 15°C/min. The added helium pressure was always set to 0.8 bar at the time of vaporisation of the sample, in order to keep constant the inlet pressure of the sample in the second gas chromatograph.

A two-position valve at the outlet of the column allowed the eluent to be directed to two different mass spectrometers: (1) a time-of-flight mass spectrometer for structural analysis of the pyrolysates or (2) through a combustion furnace and into an isotope ratio mass spectrometer.

An independent supply of helium was fitted to the fourth port of the valve to provide constant carrier gas supply to the mass spectrometer that was disconnected from the second gas chromatograph flow.

TOFMS analysis

Identification of the pyrolysates and study of the kinetics of the pyrolysis were conducted using a bespoke TOF mass spectrometer (IsoTOF, Mass Spec Solutions, Manchester, UK). The spectra of the pyrolysates were matched using the NIST library (NIST, Gaithersburg, MD, USA).

IRMS analysis

Carbon stable isotopic ratios were analysed using an IRMS instrument (Isoprime, Micromass, Manchester, UK) as the detector. For isotopic analysis, the pyrolysates were oxidised at 850°C in a combustion furnace packed with copper oxide (CuO) granules. The combustion products were then passed through a Nafion® membrane to remove water from the gas stream prior to entering the mass spectrometer.

Isotope ratios were calibrated against a CO_2 reference purchased from Air Products (Allentown, PA, USA) with a known value relative to the international isotopic reference carbonate, NBS 18. The ratios are presented using the delta notation (Eqn. (1)):

$$\delta^{13}C_{VPDB} = \left[\frac{R_{sample} - R_{VPDB}}{R_{VPDB}}\right] \times 10^3 \quad (1)$$

where $R = [^{13}C]/[^{12}C]$ and VPDB refers to the international standard Vienna PeeDee Belemnite.

Design

Evaluation of fractionation effects associated with components of the GC-Py-GC-TOFMS/c-IRMS system

It was necessary to first investigate whether the system presented mass discriminatory stages that might imply internal isotopic fractionation of the sample. The mass discriminatory processes of GC-C-IRMS and their effects have been identified and studied.[54,55] The GC-Py-GC-TOFMS/c-IRMS system, however, presents additional stages not evaluated in previous work.

The pyrolysis unit described previously presents an open-split. The split ratio created at the outlet of the furnace is flow rate dependent and is therefore a possible source of differential fractionation. Another possible source of isotopic fractionation is the distortion of the chromatographic peaks because of the increased length of the capillary. To reduce this effect, the bespoke cryo-focusing system was used to re-focus the MTBE and its pyrolysates after pyrolysis. This allowed a constant flow rate in the second GC column. Cryo-focusing is also potentially mass discriminatory. The system was tested for possible internal isotopic fractionation associated with the configuration of the system. The $\delta^{13}C$ of MTBE was analysed under the following three configurations, with a furnace temperature of 400°C which does not pyrolyse MTBE:

- Configuration 1: No cryo-focusing and a constant added helium pressure. The system was set as previously described but the sample was not cryo-focused and the

DOI: 10.1002/rcm

added helium pressure was kept constant throughout the run at 0.8 bar.
- Configuration 2: Cryo-focusing and a constant added helium pressure. The sample was cryo-focused after pyrolysis and vaporised. The added helium pressure was kept constant throughout the run at 0.8 bar.
- Configuration 3: Cryo-focusing with variable added helium pressure. The sample was cryo-focused after pyrolysis and vaporised. The added helium pressure was set at 0.3 bar during pyrolysis but increased to 0.8 bar during vaporisation.

Analyses were carried out five times for each configuration. The results of these experiments were statistically analysed using the Minitab 15 statistical package (Minitab Inc., State College, PA, USA).

Optimisation of the pyrolysis temperature

The kinetics of the pyrolysis reaction was studied for a range of temperatures between 500 and 750°C. Pyrolysis was carried out with different reaction times. Four added helium pressures between 0.1 and 0.4 bar were used to obtain a range of reaction times. Each analysis was carried out in triplicate with the TOFMS instrument as the analyser, and the uncertainty determined.

Investigation of the kinetic isotope effect associated with pyrolysis

Once the optimal pyrolysis temperature had been established, the effect of pyrolysis on the isotopic signatures of MTBE and its pyrolysates was investigated. The added helium pressure was varied between 0.2 and 0.45 bar in 0.05 bar increments to change the reaction time of the pyrolysis, and the $\delta^{13}C$ values of MTBE and the pyrolysates were measured in the IRMS instrument. Each analysis was carried out in triplicate and the error calculated.

The IRMS results were quantified using benzene as an internal standard. The major ion response in the IRMS instrument is proportional to the number of moles of CO_2 entering the ion source which in turn is related to the number of carbon atoms in the parent molecule and it may be normalised using Eqn. (2):

$$\frac{PA(X_1)}{x_1 \times n_{x_1}} = \frac{PA(X_2)}{x_2 \times n_{x_2}} \quad (2)$$

where PA(X) is the peak area of the major ion, n_x the number of moles and x the number of carbon atoms. A calibration curve was constructed using benzene as an internal standard. Various molar ratios of MTBE and benzene were analysed in triplicate using the system in configuration 3.

RESULTS AND DISCUSSION

Evaluation of fractionation effects associated with components of the GC-Py-GC-TOFMS/c-IRMS system

To investigate the fractionation effect associated with the components of the system, the $\delta^{13}C$ values of MTBE and benzene under configurations 1, 2 and 3 of the systems were measured. They are presented in Table 1. The results were compared for the two compounds using Student's unpaired two-tailed t-test analysis with a significant difference at $p = 0.05$. The results of the t-tests are shown in Table 2.

In all three configurations, there was no significant difference between the isotopic values of MTBE and benzene. The difference in split ratio in configurations 2 and 3 did not have a significant influence on the carbon isotopic values, nor did the introduction of cryo-focusing between configurations 1 and 2. The standard deviations of MTBE and benzene $\delta^{13}C$ values were poor in configuration 1 (1.5 and 0.8‰, respectively) but decreased to generally acceptable values for continuous flow stable isotope analysis (0.3 and 0.2‰. respectively), demonstrating that cryo-focusing improves the precision of the system.

Table 1 also presents the $\delta^{13}C_{VPDB}$ values of MTBE calculated with benzene as an internal reference using Eqn. (3):[57]

$$\delta^{13}C(MTBE)_{VPDB} = \delta^{13}C(benzene)_{VPDB} + \delta^{13}C(MTBE)_{benzene} + \delta^{13}C(benzene)_{VPDB} \times \delta^{13}C(MTBE)_{benzene} \quad (3)$$

While the external CO_2 reference pulses compensate only for isotopic fractionation occurring in the IRMS instrument, benzene undergoes all the mass discriminative stages in the system. Results using benzene as a reference proved to be more precise and were adopted for this work.

Optimisation of the pyrolysis temperature

The criteria for the selection of the pyrolysis conditions for on-line PSIA follow the notion of 'isotopic fidelity' introduced by Brenna and co-workers.[49–51] Isotopic fidelity describes the degree of correlation between the isotope ratio

Table 1. $\delta^{13}C$ values of MTBE and benzene in configurations 1, 2 and 3 of the system. Added helium pressure 1 (P_1) is the added helium pressure during pyrolysis and added helium pressure 2 (P_2) is the added helium pressure after vaporisation. $\delta^{13}C(MTBE)^a$ is the value calculated with the CO_2 reference gas pulses, $\delta^{13}C(MTBE)^b$ is the value calculated with benzene as internal isotopic standard following Eqn. (3) (n = number of samples, SD: standard deviation)

	Configurations									
		P_1	P_2							
Number	Cryo-focusing	(bar)		n	$\delta^{13}C$(MTBE) (‰)	SD (‰)	$\delta^{13}C$(benzene)[a] (‰)	SD (‰)	$\delta^{13}C$(MTBE)[b] (‰)	SD (‰)
1	No	0.8	0.8	6	−26.9	1.5	−25.8	0.8	−27.1	0.3
2	Yes	0.8	0.8	6	−27.6	0.3	−25.8	0.2	−27.3	0.1
3	Yes	0.8	0.3	5	−27.7	0.4	−26	0.1	−27.3	0.1

DOI: 10.1002/rcm

Table 2. Two-sample Student's t-test values comparing results from analysis using configurations 1, 2 and 3 of the system. 1vs2 means configuration 1 tested against configuration 2. MTBE[a] t-value was calculated with δ^{13}C(MTBE)[a] and MTBE[b] t-value with δ^{13}C(MTBE)[b]. The *p*-value is the probability for the two means to be equal; the hypothesis is rejected if $p \leq 0.05$. df is the degree of freedom calculated for samples with unequal variances

	df	t-value	P-value
		1vs2	
*M*TBE[a]	4	1	0.372
Benzene	4	0.08	0.942
MTBE[b]	5	1.92	0.113
		1vs3	
*M*TBE[a]	4	1.12	0.326
Benzene	4	0.45	0.675
MTBE[b]	6	1.17	0.285
		2vs3	
*M*TBE[a]	6	0.36	0.729
Benzene	7	1.24	0.254
MTBE[b]	4	−0.90	0.421

of a fragment and that of a specific moiety in the original compound.[49] An ideal fragment has a fidelity of 100%, meaning that it originates entirely from a unique position or moiety.

Preliminary work showed that MTBE pyrolysed at temperatures above 500°C and that, at temperatures above 750°C, MTBE had quantitatively reacted but showed evidence of polymerisation. Secondary reactions of the pyrolysates and polymerisation affect the fidelity. Optimisation of the pyrolysis was therefore investigated between 600 and 750°C. The progress curves of MTBE at various temperatures are presented in Fig. 3(a). The remaining fraction of MTBE (f) was calculated using Eqn. (4):

$$f = \frac{C}{C_0} = \frac{\frac{\mathrm{PA[MTBE]}}{\mathrm{PA[benzene]}}}{\frac{\mathrm{PA[MTBE]_0}}{\mathrm{PA[benzene]_0}}} \quad (4)$$

where PA[X] is the peak area of the compound X after pyrolysis and $\mathrm{PA[X]_0}$ the peak area of the compound X when the pyrolysis furnace is set at 500°C. We used the peak areas of benzene to normalise the data to compensate for the variations of the split ratio of the pyrolysis furnace.

MTBE broke down into methanol and isobutylene. Other pyrolysis products such as dimers or polymers could be detected but at negligible levels. Daly and Wentrup[58] demonstrated that the pyrolysis of MTBE at low temperatures might proceed through the *intra*molecular elimination depicted in Fig. 4. The methanol fragment originates from the methoxy group while the isobutylene originates from the 2-*methylpropane* group. At 750°C, MTBE had completely reacted and polymers could be detected only in trace amounts; however, the quantity of isobutylene detected through the TOFMS system decreased with increased residence time (Fig. 3(b)), indicating secondary pyrolysis reactions. These reactions are likely to lead to isotopic fractionation and, because the extent of this fractionation may not be known and cannot be calculated, 750°C may not be the optimal temperature for PSIA of MTBE.

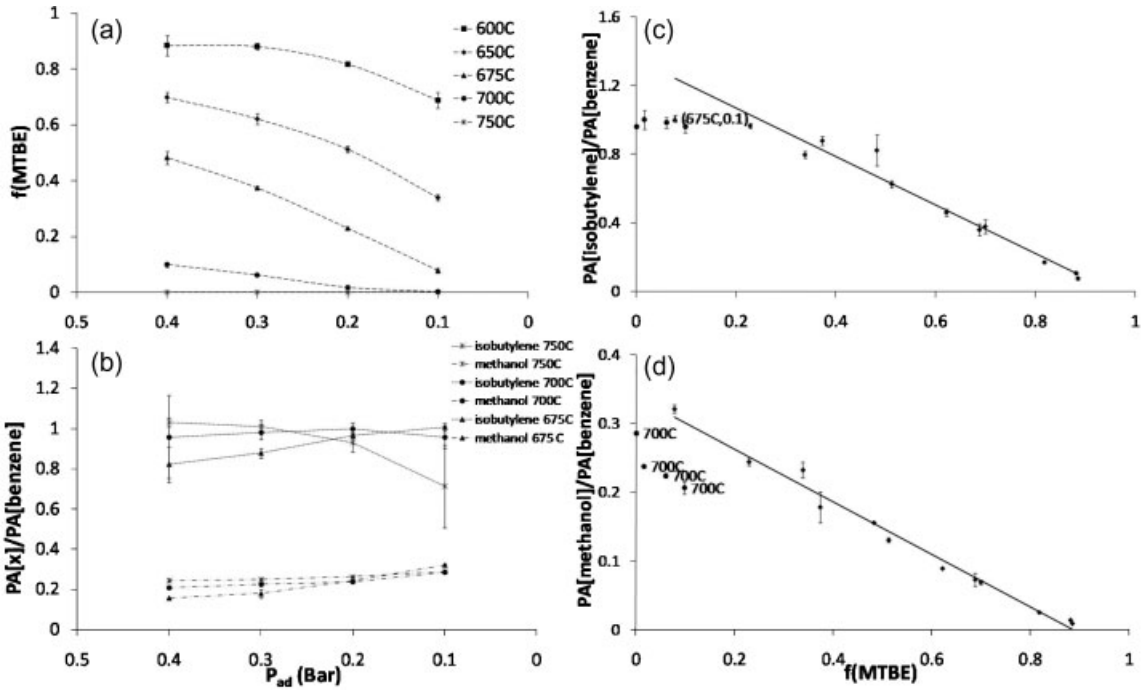

Figure 3. (a) Plot of the remaining fraction of MTBE vs. the added helium pressure (P_{ad}) at various temperatures. (b) Plot of the quantity of the pyrolysates vs. P_{ad} at 675°C, 700°C and 750°C. (For plots (a) and (b) the P_{ad} values are in reverse order to simulate a residence time scale.) (c) Quantity of isobutylene vs. remaining fraction of MTBE. (d) Quantity of methanol vs. remaining fraction of MTBE. (The quantity of the pyrolysates in plots (b), (c) and (d) are expressed as the ratio of their peak area over the peak area of benzene.)

DOI: 10.1002/rcm

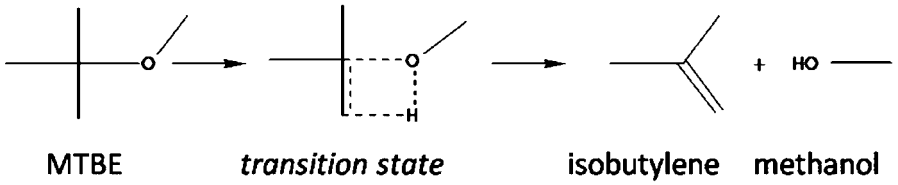

Figure 4. Mechanism of the pyrolysis of MTBE.

For temperatures up to and including 675°C, the formation of isobutylene and methanol followed the kinetics of the consumption of MTBE (Figs. 3(b), 3(c) and 3(d)) but, at 700°C, the concentration of the pyrolysates was lower than that of the MTBE reacted, indicating that secondary pyrolysis reactions had started. A temperature of 675°C was thus chosen as the optimal pyrolysis temperature for the PSIA of MTBE because, at this temperature, for all added helium pressures studied, the yield of the reaction is high (f ranges from 0.40 to 0.07), the fidelity of both pyrolysates is 100% and the pyrolysates are not involved in secondary reactions.

Investigation of the kinetic isotope effect associated with pyrolysis

The Rayleigh equation

We established that there was no fractionation associated with the inherent process of the system; however, because the reaction is not quantitative at the chosen pyrolysis temperature, 675°C, it is likely that isotopic fractionation will occur during pyrolysis. In effect, the pyrolysis of MTBE within this system is believed to occur through a molecular elimination reaction during which a C–O bond is broken. Heavier isotopes of an atom form more stable chemical bonds than lighter isotopes of the same atom; hence a ^{13}C–O bond will require more energy to break than a ^{12}C–O bond. As pyrolysis reactions involve the cleavage of bonds, they are therefore likely to be sensitive to the atomic mass resulting in a kinetic isotope effect. The remaining MTBE will be enriched in ^{13}C while the weighted average ratios of the products of pyrolysis will be depleted compared with that of the original MTBE. The enrichment undergone by the MTBE during the pyrolysis may be quantified using the following version of the Rayleigh equation as developed by Mariotti *et al.*:[59]

$$\ln(\delta^{13}\mathrm{C(MTBE)}_{\mathrm{rem}}+1000)=\frac{\varepsilon_{\mathrm{R}}}{1000}\cdot\ln f+\ln(\delta^{13}\mathrm{C}_0+1000) \quad (5)$$

where $\delta^{13}C_0$ and $\delta^{13}C(MTBE)_{rem}$ are the carbon isotopic signatures of MTBE before and after pyrolysis, respectively, f the remaining fraction of MTBE after pyrolyis and ε_R the enrichment factor.

Determination of the remaining fraction of MTBE

To construct the Rayleigh plot, quantification of the remaining fraction of MTBE in the IRMS instrument is required. A calibration curve was produced using benzene as an internal standard. Figure 5 presents a plot of the ratio of the major ion peak areas of MTBE and benzene vs. the molar ratio of the injected solutions. According to Eqn. (2), the theoretical equation of this curve is $y=\frac{5}{6}x$. The experimental curve presented a linear fit and the value of its slope was close to 5/6. The good fit showed that, for the range of concentrations studied, the major ion response was linear and that it could be used for quantification by means of Eqn. (2). The linear fit was demonstrated only for the relationship between MTBE and benzene, but the assumption was made that Eqn. (2) may also be used for quantification of isobutylene and methanol.

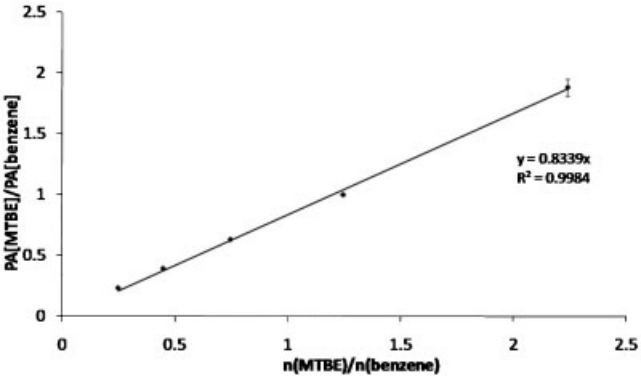

Figure 5. Calibration curve for the quantification of MTBE in the IRMS system. Benzene was used as an internal standard (error bars represent 1 standard deviation).

The pre-pyrolysis fractionation

Figure 6(a) presents the Rayleigh plot for the pyrolysis of MTBE at 675°C constructed with the quantified f values and the $\delta^{13}C_{VPDB}$(MTBE) values obtained for the various added helium pressures. By linear regression, the enrichment factor was found to be −1.71 and the $\delta^{13}C_0$, calculated using the origin ordinate, was −26.4‰ with a 95% confidence interval of 0.4‰. This value for $\delta^{13}C_0$, the carbon isotopic signature of MTBE before pyrolysis, is different from the δ^{13}C(MTBE) determined analytically at 500°C (−27.3‰). To verify whether this difference in the calculated and analytical values for δ^{13}C(MTBE) is a real isotopic shift or a mathematical artefact a total mass balance of carbon atoms was calculated for each added helium pressure according to Eqn. (6):

$$\begin{aligned}\delta^{13}\mathrm{C(tot)} = {} & (\chi_{\mathrm{MTBE}}\times\delta^{13}\mathrm{C(MTBE)}_{\mathrm{rem}}) \\ & +(\chi_{\mathrm{methanol}}\times\delta^{13}\mathrm{C(methanol)}) \\ & +(\chi_{\mathrm{isobutylene}}\times\delta^{13}\mathrm{C(isobutylene)})\end{aligned} \quad (6)$$

with $\chi_x=\frac{\mathrm{PA(X)}}{\sum \mathrm{PA}}$; δ^{13}C(tot), the total mass balance of the δ^{13}C values; and δ^{13}C(methanol) and δ^{13}C(isobutylene), the measured $\delta^{13}C_{VPDB}$ values of methanol and isobutylene, respectively, using benzene as internal standard.

DOI: 10.1002/rcm

RCM

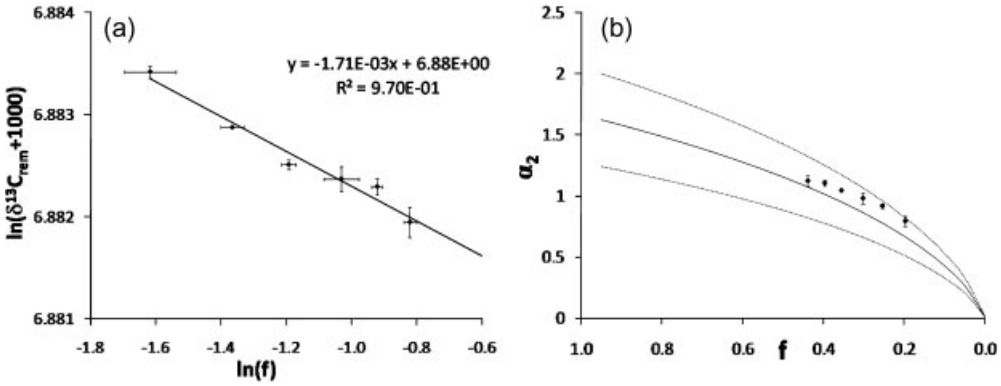

Figure 6. (a) Rayleigh plot of the pyrolysis of MTBE at 675°C. (b) Curve of the calculated enrichment α_2 of the accumulated products of the pyrolysis vs. the remaining fraction of MTBE. Dashed point curves are the 95% confidence interval curves; the diamonds represent the experimental values of α_2. (The error bars represent the 95% confidence interval.)

Table 3. Results for the total mass balance (δ^{13}C(tot)), α_1, α_2 and the absolute δ^{13}C values of the two functional groups of MTBE at various added helium pressures (CI: confidence interval)

P_{ad} (bar)	f	δ^{13}C(tot) (‰)	CI (95%)	α_1 (‰)	CI (95%)	α_2 (‰)	CI (95%)	δ^{13}C(methoxy) (‰)	CI (95%)	δ^{13}C(2-methylpropane) (‰)	CI (95%)
0.45	0.44	−26.4	0.1	−0.9	0.4	1.1	0.3	−35.4	0.4	−25.3	0.5
0.40	0.40	−26.3	0.2	−0.9	0.4	1.0	0.3	−35.4	0.4	−25.3	0.5
0.35	0.36	−26.4	0.1	−0.9	0.4	1.0	0.3	−35.2	0.4	−25.4	0.5
0.30	0.30	−26.6	0.1	−0.9	0.4	0.9	0.2	−35.3	0.4	−25.7	0.5
0.25	0.26	−26.6	0.1	−0.9	0.4	0.8	0.2	−35.3	0.4	−25.7	0.5
0.20	0.20	−26.7	0.1	−0.9	0.4	0.7	0.2	−35.2	0.4	−25.8	0.5

The results for the δ^{13}C(tot) and their 95% confidence intervals at the various added helium pressures are presented in Table 3. These values (between −26.3 and −26.7‰) are similar to the $\delta^{13}C_0$ value obtained from the Rayleigh plot regression but are significantly different from the δ^{13}C(MTBE) value determined at 500°C. Matter conservation dictates that δ^{13}C(tot) is equal to the δ^{13}C value of MTBE before the start of the pyrolysis reaction. These results therefore indicate that the difference between the values of δ^{13}C(MTBE) and $\delta^{13}C_0$ is not a mathematical artefact but does in fact represent a carbon isotopic shift of MTBE between the moment it enters the system and the beginning of pyrolysis. Moreover, the δ^{13}C(tot) values do not appear to vary significantly for the various added helium pressures, suggesting that the isotopic fractionation undergone by MTBE prior to pyrolysis does not depend on the residence time of MTBE in the pyrolysis furnace. We named this 'pre-pyrolysis' fractionation α_1, where $\alpha_1 = \delta^{13}$C(MTBE) − $\delta^{13}C_0 = -0.9$‰.

Kinetic isotopic fractionation of the pyrolysates

The Rayleigh plot demonstrated that the pyrolysis reaction is a mass-selective process. When the reaction is not complete, the isotopic signature of the reaction products is representative only of the reacted MTBE. Mariotti *et al.*[59] proposed an equation for the calculation of the average accumulated products isotopic ratio in a non-quantitative chemical reaction (Eqn. (7)):

$$\frac{\delta^{13}C_{pyro} + 1000}{\delta^{13}C_0 + 1000} = \frac{1}{(1-f)} \cdot \left[1 - f^{1+\frac{\varepsilon_R}{1000}}\right] \quad (7)$$

where $\delta^{13}C_{pyro}$ is the weighted average δ^{13}C of the accumulated products. Therefore, for the pyrolysis of MTBE:

$$\delta^{13}C_{pyro} = \frac{4}{5} \times \delta^{13}\text{C(isobutylene)} + \frac{1}{5} \times \delta^{13}\text{C(methanol)} \quad (8)$$

Equation (7) may be rearranged to calculate the total fractionation, α_2, of the pyrolysates:

$$\alpha_2 = \delta^{13}C_0 - \delta^{13}C_{pyro} = \frac{f}{1-f} \cdot \left(f^{1+\frac{\varepsilon_R}{1000}} - 1\right) \cdot \left(\delta^{13}C_0 + 1000\right) \quad (9)$$

Figure 6(b) presents the theoretical curve of α_2 calculated from the right-hand term of Eqn. (9) using $\delta^{13}C_0$ and ε_R obtained from the Rayleigh plot regression. To test the model vs. the experimental data, an experimental value of α_2 was obtained, for each analysis, by determining $\delta^{13}C_{pyro}$ and substituting $\delta^{13}C_0$ by δ^{13}C(tot). The experimental α_2 values are also presented in Fig. 6(b) for comparison; they all fall within the 95% confidence interval of the theoretical curve.

The Rayleigh plot has therefore enabled us to determine the existence of a pre-pyrolysis depletion and to calculate the

DOI: 10.1002/rcm

total isotopic shift between the fragments and the parent molecule. The 'pre-pyrolysis' enrichment can be evaluated experimentally by comparing the $\delta^{13}C$(tot) resulting from the mass balance and the $\delta^{13}C$ value of the parent MTBE determined either by compound-specific analysis or using the PSIA system with a non-pyrolysing temperature for the pyrolysis furnace. The second enrichment, α_2, is due to the pyrolysis reaction and can be evaluated from Eqn. (9) using the parameters from the Rayleigh plot regression.

Determination of the correction factors linking pyrolysates and their parent moieties

The total correction, $\alpha_1 + \alpha_2$, links $\delta^{13}C$(MTBE) and $\delta^{13}C_{pyro}$. We aim, however, to access the individual carbon isotopic signature of the two functional groups of MTBE. This is possible by making the two following assumptions: (1) the 'pre-pyrolysis' fractionation is homogeneous, thus α_1 is equally distributed for the five MTBE carbon atoms. The assumption was made on the premise that the isotopically selective process that MTBE appears to undergo before pyrolysis was physical rather than chemical and therefore would not occur on a particular moiety in the molecule. (2) As described previously, and presented in Fig. 4, the mechanism of the pyrolysis of MTBE is a molecular elimination, occurring with the breaking of the C−O ether bond on the 2-methylpropane side of the molecule. For carbon kinetic isotopic fractionation in chemical reactions, the secondary isotopic effects (effects on the carbon atoms that are not involved in the chemical reactions) are usually negligible and isotopic fractionation is noticeable only on the carbon atoms undergoing the reaction. Thus, because the primary fractionation occurs only on the carbon atoms of the 2-methylpropane group, the carbon isotopic signature of the methoxy group should not be affected by the pyrolysis. This assumption ideally should have been verified by the evolution of the $\delta^{13}C$ values of methanol and isobutylene during pyrolysis. Theoretically, the methanol values should have remained constant and the isobutylene values should have changed as a function of the progress of the reaction. In the range of progress of the reaction obtained here (f values between 0.20 and 0.44), however, the difference between lowest and highest values of α_2 is only 0.4‰, which is only slightly above the system precision and no significant differences could be observed for the $\delta^{13}C$ values of isobutylene at the various stages of the reaction.

Following the two preceding assumptions, $\delta^{13}C$(methoxy) and $\delta^{13}C$(2-methylpropane) were calculated according to Eqns. (10) and (11), respectively. In Eqn. (10), the factor 5/4 was introduced before α_2 to compensate for the dilution effect in the calculation of $\delta^{13}C_{pyro}$.

$$\delta^{13}C(\text{methyoxy}) = \delta^{13}C(\text{methanol}) + \alpha_1 \quad (10)$$

$$\delta^{13}C(\text{tert}-\text{butyl}) = \delta^{13}C(\text{isobutylene}) + \alpha_1 + \frac{5}{4}\alpha_2 \quad (11)$$

The values for $\delta^{13}C$(methoxy) and $\delta^{13}C$(2-methylpropane) are presented in Table 3 for the various added helium pressures. These values are absolute and can be presented against the international standard VPDB.

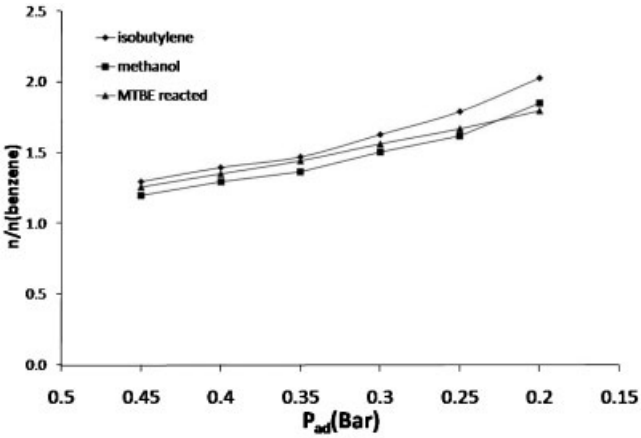

Figure 7. Molar quantities of the two pyrolysates and the MTBE reacted vs. the added helium pressure.

The results for $\delta^{13}C$(methoxy) do not show significant differences for the various residence times; the results for $\delta^{13}C$(2-methylpropane), however, appear slightly depleted for the lowest added helium pressures (Table 3). Figure 7 shows the change in concentration of the two pyrolysates and reacted MTBE with residence time. For the shortest residence times, the concentrations of methanol, isobutylene and reacted MTBE were very similar. For longer residence times, however, the apparent concentration of isobutylene became much higher than that of the reacted MTBE. When the sample resides for a long time in the furnace at high temperature prior to being cryo-focused, it is possible that impurities accumulate. Isobutylene was the first eluted compound from the second gas chromatograph; unretained impurities might co-elute with it, creating the appearance of a higher concentration and influencing the carbon isotope signature. The routine operational settings, however, can be established to exclude these minor effects by choosing an optimal added helium pressure, higher than 0.3 bar.

Robustness of the system

The reliability of the system depends on the reproducibility of the results. It is therefore important to evaluate how variations of the system set-up could affect its robustness. The pre-pyrolysis fractionation, α_1, appears to be caused by the elevated temperature of the pyrolysis, given that the only change made to the system between the determination of $\delta^{13}C$(MTBE) and that of $\delta^{13}C$(tot) was the pyrolysis furnace temperature. Its extent was found not to depend on the residence time of the sample in the furnace but is, however, likely to be proportional to the $\delta^{13}C$ value of the parent MTBE sample. It is, thus, necessary to evaluate experimentally its value for individual samples as described previously. The second fractionation, α_2, depends on the parameters of the Rayleigh plot regression, ε_R and $\delta^{13}C_0$, and on the progress of the reaction. The enrichment factor, ε_R, will not change as long as the pyrolysis temperature remains constant as it is a factor of the kinetics of the reaction. $\delta^{13}C_0$ depends on the $\delta^{13}C$ value of the parent MTBE and on the pre-pyrolysis enrichment but is experimentally determined by $\delta^{13}C$(tot).

DOI: 10.1002/rcm

Finally, the progress of the reaction is a sole function of the residence time, which in turn depends on the flow rate and the volume of the pyrolysis furnace. The characteristics of the pyrolysis furnace that dictate the flow rate are the added helium pressure and the dimension of the outlet split; the volume is determined by the length and diameter of the quartz tube and the length of fused-silica capillaries inserted into the furnace on both sides. When no changes are made to these parameters and f, the remaining fraction of MTBE in the optimal pysolysis conditions, is known, α_2 can be calculated for each analysis using Eqn. (9). In a case where changes were made, it would be necessary to recalculate f in the optimal pyrolysis conditions, prior to the determination of α_2, according to Eqn. (4) and using benzene as the internal standard.

CONCLUSIONS

We successfully designed an advanced system for the routine analytical determination of intramolecular isotope signatures. Variable pyrolysis reaction times and use of an internal reference provided us with the tools for a greater understanding of the real fractionations associated with the inherent nature of the process. We first were able to rule out any fractionation associated with the additional features of the system, i.e. the additional open-split and the cryo-focusing. For MTBE, we identified two types of fractionations undergone by the compound of interest during pyrolysis; a pre-pyrolysis depletion and the kinetic isotope effect of the pyrolysis reaction. This enabled us to produce absolute values for the $\delta^{13}C$ of individual moieties in the molecule that can be presented against the international standard VPDB. Interlaboratory comparisons have therefore become theoretically possible for the on-line PSIA of MTBE. MTBE was a straightforward case for the development of an on-line position-specific isotope analysis system because the mechanism of the pyrolysis of MTBE at temperatures below 700°C follows a unique route of molecular elimination and both pyrolysates have an isotopic fidelity of 100%. On-line PSIA of molecules of interest with several simultaneous pyrolysis mechanisms and isotopic fidelities different from 100% might involve more complex calculations for the isotopic correction factors.

The method will provide a useful tool for source tracking of MTBE and many other contaminants of concern in the environment, and potentially to uniquely identify discrete microbial utilisation pathways. For instance, in the case of MTBE, both functional groups are possible sites of attack during biodegradation; monitoring the changes in their $\delta^{13}C$ values should give insight into the first steps of the degradation mechanisms.

Acknowledgements

The authors would like to thank Neil Wallace for invaluable technical support and advice. Mass Spec Solutions (Manchester, UK) is acknowledged for constant assistance to the project. The work was financially supported by the EPSRC grant EP/D013739/1 (PhD studentship for CG), the Queen's University of Belfast and the University of Strathclyde, Glasgow.

REFERENCES

1. Sano M, Yotsui Y, Abe H, Sasaki S. *Biomed. Mass Spectrom.* 1973; **3**: 1.
2. Matthews DE, Hayes JM. *Anal. Chem.* 1978; **50**: 1465.
3. Barrie A, Bricout J, Koziet J. *Biol. Mass Spectrom.* 1984; **11**: 583.
4. Hall JA, Barth JAC, Kalin RM. *Rapid Commun. Mass Spectrom.* 1999; **13**: 1231.
5. Meier-Augenstein W. *J. Chromatogr. A* 1999; **842**: 351.
6. Hayes JM, Freeman KH, Popp BN, Hoham CH. *Org. Geochem.* 1990; **16**: 1115.
7. Jasper JP, Westenberger BJ, Spencer JA, Buhse LF, Nasr M. *JPBA* 2004; **35**: 21.
8. Morrison DJ, Cooper K, Waldron S, Slater S, Weaver LT, Preston T. *Rapid Commun. Mass Spectrom.* 2004; **18**: 2593.
9. Benson S, Lennard C, Maynard P, Roux C. *Forensic Sci. Int.* 2006; **157**: 1.
10. Slater GF. *Environ. Forensics* 2003; **4**: 13.
11. Jeffrey AWA. Application of stable isotope ratios in spilled oil identification. In *Oil Spill Environmental Forensics – Fingerprinting and Source Identification*, Wang Z, Stout SA (eds). Academic Press: New York, 2007; 207.
12. Dempster HS, Sherwood Lollar B, Feenstra S. *Environ. Sci. Technol.* 1997; **31**: 3193.
13. Smallwood BJ, Philp RP, Burgoyne TW, Allen JD. *Environmental Forensics* 2001; **2**: 215.
14. O'Sullivan G, Kalin RM. *Environ. Forensics* 2008; **9**: 166.
15. Poulson SR, Drever JI. *Environ. Sci. Technol.* 1999; **33**: 3689.
16. Harrington RR, Poulson SR, Drever JI, Colberg PJS, Kelly EF. *Org. Geochem.* 1999; **30**: 765.
17. Huang L, Sturchio NC, Abrajano T, Heraty LJ, Holt BD. *Org. Geochem.* 1999; **30**: 777.
18. Wang Y, Huang Y. *Org. Geochem.* 2001; **32**: 991.
19. Slater GF, Dempster HS, Sherwood Lollar B, Ahad J. *Environ. Sci. Technol.* 1999; **33**: 190.
20. Slater GF, Ahad JME, Sherwood Lollar B, Allen-King R, Sleep B. *Anal. Chem.* 2000; **72**: 5669.
21. Schüth C, Taubald H, Bolaño N, Maciejczyk K. *J. Contaminant Hydrol.* 2003; **64**: 269.
22. Gray JR, Lacrampe-Couloume G, Gandhi D, Scow KM, Wilson RD, Mackay DM, Sherwood Lollar B. *Environ. Sci. Technol.* 2002; **36**: 1931.
23. Hall JA, Kalin RM, Larkin MJ, Allen CCR, Harper DB. *Org. Geochem.* 1999; **30**: 801.
24. Hirschorn SK, Dinglasan MJ, Elsner M, Mancini SA, Lacrampe-Couloume G, Edwards EA, SherwoodLollar B. *Environ. Sci. Technol.* 2004; **38**: 4775.
25. Hunkeler D, Butler BJ, Aravena R, Barker JF. *Environ. Sci. Technol.* 2001; **35**: 676.
26. Kolhatkar R, Kuder T, Philp P, Allen J, Wilson JT. *Environ. Sci. Technol.* 2002; **36**: 5139.
27. Kuder T, Wilson JT, Kaiser P, Kolhatkar R, Philp P, Allen J. *Environ. Sci. Technol.* 2005; **39**: 213.
28. Mancini SA, Lacrampe-Couloume G, Jonker H, van Breukelen BM, Groen J, Volkering F, Sherwood Lollar B. *Environ. Sci. Technol.* 2002; **36**: 2464.
29. Meckenstock RU, Morasch B, Griebler C, Richnow HH. *J. Contaminant Hydrol.* 2004; **75**: 215.
30. Miller LG, Kalin RM, McCauley SE, Hamilton JTG, Harper DB, Millet DB, Oremland RS, Goldstein AH. *Proc. Natl. Acad. Ssi.* 2001; **98**: 5833.
31. Richnow HH, Annweiler E, Michaelis W, Meckenstock RU. *J. Contaminant Hydrol.* 2003; **65**: 101.
32. Rosell M, Barcelo D, Rohwerder T, Breuer U, Gehre M, Richnow HH. *Environ. Sci. Technol.* 2007; **41**: 2036.
33. Schmidt TC. *TrAC Trends Anal. Chem.* 2003; **22**: 776.
34. Schmidt TC, Schirmer M, Weiß H, Haderlein SB. *J. Contaminant Hydrol.* 2004; **70**: 173.
35. Somsamak P, Richnow HH, Haggblom MM. *Environ. Sci. Technol.* 2005; **39**: 103.
36. Somsamak P, Richnow HH, Haggblom MM. *Appl. Environ. Microbiol.* 2006; **72**: 1157.
37. Barth JAC, Slater G, Schuth C, Bill M, Downey A, Larkin M, Kalin RM. *Appl. Environ. Microbiol.* 2002; **68**: 1728.
38. Elsner M, Zwank L, Hunkeler D, Schwarzenbach RP. *Environ. Sci. Technol.* 2005; **39**: 6896.
39. Zwank L, Berg M, Elsner M, Schmidt TC, Schwarzenbach RP, Haderlein SB. *Environ. Sci. Technol.* 2005; **39**: 7344.

DOI: 10.1002/rcm

40. Fischer A, Herklotz I, Herrmann S, Thullner M, Weelink SAB, Stams AJM, Schlömann M, Richnow H, Vogt C. *Environ. Sci. Technol.* 2008; **42**: 4356.
41. O'Sullivan G. *PhD thesis*, Queen's University Belfast, 2004.
42. Elsner M, McKelvie J, Lacrampe Couloume, Sherwood Lollar B. *Environ. Sci. Technol.* 2007; **41**: 5693.
43. Abelson PH, Hoering TC. *Proc. Natl. Acad. Sci.* 1961; **47**: 623.
44. Vogler EA, Hayes JM. *J. Org. Chem.* 1979; **44**: 3682.
45. Monson KD, Hayes JM. *Geochim. Cosmochim. Acta* 1982; **46**: 139.
46. Corso TN, Brenna JT. *Proc. Natl. Acad. Sci.* 1997; **94**: 1049.
47. Corso TN, Brenna JT. *Anal. Chim. Acta* 1999; **397**: 217.
48. Corso TN, Lewis BA, Brenna JT. *Anal. Chem.* 1998; **70**: 3752.
49. Wolyniak CJ, Sacks GL, Metzger SK, Brenna JT. *Anal. Chem.* 2006; **78**: 2752.
50. Wolyniak CJ, Sacks GL, Pan BS, Brenna JT. *Anal. Chem.* 2005; **77**: 1746.
51. Sacks GL, Brenna JT. *Anal. Chem.* 2003; **75**: 5495.
52. Yamada K, Tanaka M, Nagawa F, Yoshida N. *Rapid Commun. Mass Spectrom.* 2002; **16**: 1059.
53. Dias RF, Freeman KH, Franks SG. *Org. Geochem.* 2002; **33**: 161.
54. Merritt DA, Brand WA, Hayes JM. *Org. Geochem.* 1994; **21**: 573.
55. Meier-Augenstein W. GC and IRMS technology for 13C and 15N analysis on organic compounds and related gases. In *Handbook of Stable Isotope Analytical Techniques*, de Groot PA (ed). Elsevier: Amsterdam, 2004; 171.
56. Nesbitt ER, Robinson C, Cantrell RL, Foresco CB, Lahey K, Tortorice J. *Methyl tertiary-Butyl Ether (MTBE): Conditions Affecting the Domestic Industry*, US International Trade Commission, Washington DC 20436, 1999.
57. Coplen TB. *Pure Appl. Chem.* 1994; **66**: 273.
58. Daly NJ, Wentrup C. *Aust. J. Chem.* 1968; **21**: 2711.
59. Mariotti A, Germon J, Hubert P, Kaiser P, Letolle R, Tardieux A, Tardieux P. *Plant Soil* 1981; **62**: 413.

DOI: 10.1002/rcm